# Multistability and localized attractors in a dissipative discrete NLS equation

Panayotis Panayotaros, Felipe Rivero
Depto. Matemáticas y Mecánica
I.I.M.A.S.-U.N.A.M.
Apdo. Postal 20–726, 01000 México D.F., México
Tel.(55) 5622-3600, Fax (55) 5622-3564
e-mail: panos@mym.iimas.unam.mx
lfeliperiverog@mym.iimas.unam.mx

June 27, 2013

**Abstract**

We consider a finite discrete nonlinear Schrödinger equation with localized forcing, damping, and nonautonomous perturbations. In the autonomous case these systems are shown numerically to have multiple attracting spatially localized solutions. In the nonautonomous case we study analytically some properties of the pullback attractor of the system, assuming that the origin of the corresponding autonomous system is hyberbolic. We also see numerically the persistence of multiple localized attracting states under different types of nonautonomous perturbations.

## 1 Introduction

We study some properties of attractors of a finite discrete nonlinear Schrödinger (DNLS) system with dissipation, localized forcing, and nonautonomous perturbations. The dynamics of the autonomous dissipative DNLS system exhibits spatial localization and multistability, and we also examine these phenomena in the presence of nonautonomous perturbations, applying some recent notions of attractivity for nonautonomous dissipative systems.

The DNLS system we consider is a basic model for coupled waveguide arrays in optics [5], and there are several physically realizable mechanisms of dissipation and gain. We here consider the standard cubic DNLS with a linear term that describes linear dissipation or gain at each site, as well as a cubic dissipative saturation term. The linear part generalizes the non-Hamiltonian and non-Hermitian linear part of PT-symmetric discrete NLS equations proposed in [16], while the nonlinear dissipative term leads to the existence a global attractor. The resulting system is also a discrete 1-D version of the spatially forced dissipative NLS equation considered in [10], see the related localized gain models of [11], [15]. In these models the mathematical time variable represents distance along the optical axis. The nonautonomous perturbation is of additive type, and could model energy "kicks" at different regions along an optical fiber, unequal or noisy "kicks"

at equally spaced regions of the fiber, and other types of external forcing, e.g. through an input coupler. Perturbations of the system parameters are generally more interesting since they also depend on the signal, but are not considered here mainly for mathematical simplicity. We believe however that they can be eventually included in the framework of sections 2, and 3.

The long time behavior of the autonomous dissipative DNLS system is characterized by its attractor. In the presence of nonautonomous perturbations we also show that the system has a pullback attractor. The notion of a pullback attractor, see [1], is a generalization of the notion of an attractor, applicable to general nonautonomous systems. A recent exposition of the theory can be found in [4]. Roughly, a section (or "slice") $\mathscr{A}(t)$ of a pullback attractor at time $t$ contains all possible states observed at time $t$ of a physical process that had started at past time $t_0$, with $t_0 \to -\infty$. Information on the detailed structure of the pullback attractor has been so far obtained for nonautonomous perturbations of wave systems with relatively simple dynamics, e.g. the damped nonlinear wave equations studied in [1], [2]. The proposed equation is a simple model that shows more complicated dynamics and motivates further work on these problems.

To obtain information on the geometric structure of the attractor we use a combination of analytical arguments and numerics. In the case where the origin is a hyperbolic fixed point of the autonomous system we use results of [3] to see that the pullback attractor of the nonautonomous perturbation includes nonautonomous analogues of the hyperbolic fixed point and its local unstable manifold. The condition of hyperbolicity at the origin can be verified theoretically for small intersite coupling, and we also see numerically that it can hold in the presence of strong intersite coupling.

For small intersite coupling the dynamics and spatial localization pattern of the asymptotic states of the system contained in the attractor is largely determined by the spatial structure of the linear forcing and damping term, and we see localization at the forced sites. Increasing the coupling strength leads to more complicated spatial localization patterns, and multistability. We also see evidence of asymptotic states that are likely not periodic. Their localized structure also persists under different nonautonomous perturbations, although the nonautonomous forcing changes the basins of attraction.

The paper is organized as follows. In Section 2 we define the nonautonomous dissipative DNLS model, introduce some basic notions of attractivity for nonautonomous systems, and prove the existence of a pullback attractor. In Section 3 we prove some basic results on the invariant sets of nonautonomous perturbations of the dissipative DNLS system under the assumption of hyperbolicity of the origin. In Section 4 we give numerical examples of attractors for the autonomous and nonautonomous DNLS system, and provide evidence for the existence of multiple spatially localized attracting states.

## 2 Discrete NLS in a finite lattice and pullback attractors

We study a discrete forced and damped cubic NLS equation in a finite lattice $J = \{1, \dots, N\}$, written as

$$\frac{d}{dt}u = (iC + V)u + F(u) + G(t), \tag{1}$$

where $u = [u_1, \ldots, u_N] \in \mathbb{C}^N$,

$$(Cu)_j = -\delta u_j + \gamma(u_{j+1} + u_{j-1}), \quad \forall j \in J \setminus \{1, N\},$$
$$(Cu)_1 = -\delta u_1 + \gamma u_2, \quad (Cu)_N = -\delta u_N + \gamma u_{N-1},$$
$$(Vu)_j = V_j u_j,$$
$$(F(u))_j = (-\varepsilon + ib)|u_j|^2 u_j, \quad (G(t))_j = g_j(t), \quad \forall j \in J.$$

Parameters $\gamma$, $\delta$, $\varepsilon$, $b$ are real, and with $\varepsilon > 0$. Also $V_j \in \mathbb{R}$ and we assume that

$$|g_j(t)|^2 \leq K_j, \quad \forall t \in \mathbb{R}, \quad \forall j \in J. \tag{2}$$

The term $iC$ describes nearest neighbor coupling between the sites. For $\delta = 2\gamma$, $C$ is a discrete analogue of the Dirichlet Laplacian on the interval.

The term $(Vu)_j$ desribes forcing ($V_j > 0$) or damping ($V_j < 0$) at the site $j$. We denote the set of sites $j \in J$ satisfying $V_j > 0$ by $J_+$, and the set of sites $j \in J$ satisfying $V_j < 0$ by $J_-$.

The linear operator $iC + V$ is in general non-Hermitian and non-Hamiltonian. For $V_j = -V_{-j}$ it belongs to the class of PT-symmetric operators, see e.g. [16], and the origin can be elliptic, although in sections 3 and 4 we are interested in the case where the origin is hyperbolic.

The nonlinear term $F(u)$ contains Hamlitonian and dissipative parts. In the case where $iC+V$ is PT-symmetric, the nonlinear dissipation term is not, but it may be interesting in the PT-symmetry context as it provides a mechanism for saturation, and leads to the existence of attractors (see below).

$G(t)$ is the nonautonomous forcing term. The case $G \equiv 0$ will be referred to as the autonomous case. Note that in the autonomous case system (1) is equivariant under global phase change $u_n \mapsto e^{i\theta} u_n$, but the power $P = \sum_{j=1}^N |u_j|^2$ is not conserved.

We now consider some basic dissipativity properties of (1).

We let $X = \mathbb{C}^N = \mathbb{R}^{2N}$, with the Euclidean norm $\|\cdot\|_X$. We will also assume that $G : \mathbb{R} \to \mathbb{C}^N$ is Hölder continuous in $\mathbb{R}$.

The existence of a local solution $u(t, s; u(s)) = \{u_j(t, s; u(s))\}_{j \in J}$ of (1) with initial data $u(s) \in X$ (see, for example [9]) is immediate from the fact that $G(t)$ is Hölder continuous and the fact that the non-linearity $F(u)$ is locally Lipschitz in $X$, in fact, taking $x, y$ inside a ball of radius $R$ around the origin in $\mathbb{C}^N$,

$$\|F(x) - F(y)\|_X \leq \sqrt{3}(\varepsilon^2 + b^2)R\|x - y\|_X. \tag{3}$$

In the autonomous case, system (1) has a compact attractor. This follows from the fact that the norm $\|u(t)\|_X$ of the solution $u(t)$ satisfies

$$\frac{d}{dt}\|u\|_X^2 = 2\sum_{j \in J} \left(V_j|u_j|^2 - \varepsilon|u_j|^4\right) \leq -2\alpha\|u_j\|_X^2 + 2\sum_{j \in J} \left((V_j + \alpha)|u_j|^2 - \varepsilon|u_j|^4\right), \tag{4}$$

where $\alpha = \max\{|V_j| : j \in J^-\}$. Then

$$\frac{d}{dt}\|u\|_X^2 \leq -2\alpha\|u_j\|_X^2 + \frac{\|V_j + \alpha\|_X^2}{2\varepsilon},$$

using the fact that $-ax^2 + bx \leq \frac{b^2}{4a}$, $\forall x \in \mathbb{R}$. By Gronwall's Lemma and calling K=$\frac{\|V_j+\alpha\|_X^2}{2\varepsilon}$,

$$\|u\|_X^2 \leq \|u_s\|_X^2 e^{-2\alpha(t-s)} + K. \tag{5}$$

Therefore, there exists a ball in $X$ with radius $K$ which absorbs any solution $u(t, s; u_s)$ of (1). This ball is clearly compact. By the theory of global attractors (see [7]), there exists a compact invariant set that attracts all bounded sets of $X$.

For the nonautonomous case we recall some basic definitions and results on pullback attractors and evolution processes, see [1, 2, 4].

**Definition 2.1** *An* evolution process *in a metric space $(\mathcal{X}, d_{\mathcal{X}})$ is a family of continuous maps $\{S(t,s) : t \geq s\}$ from $\mathcal{X}$ into itself with the following properties*

1) $S(t,t) = I$, *for all* $t \in \mathbb{R}$,
2) $S(t,s) = S(t,\tau)S(\tau,s)$, *for all* $t \geq \tau \geq s$,
3) $\{(t,s) \in \mathbb{R}^2 : t \geq s\} \times \mathcal{X} \ni (t,s,x) \mapsto S(t,s)x \in \mathcal{X}$ *is continuous.*

For $A$, $B$ subsets of $\mathcal{X}$ let $\operatorname{dist}(A,B) = \sup_{a\in A} \inf_{b\in B} d_{\mathcal{X}}(a,b)$, i.e. $\operatorname{dist}(A,B)$ denotes the Hausdorff semidistance between $A$, $B$.

**Definition 2.2** *A set $B(t) \subset \mathcal{X}$* pullback attracts a set $C$ at time $t$ *under $\{S(t,s) : t \geq s\}$ if*

$$\lim_{s\to-\infty} dist(S(t,s)C, B(t)) = 0.$$

*A family $\{B(t) : t \in \mathbb{R}\}$* pullback attracts bounded subsets of $\mathcal{X}$ *under $\{S(t,s) : t \geq s\}$ if $B(t)$ pullback attracts bounded subsets at time $t$ under $\{S(t,s) : t \geq s\}$, for each $t \in \mathbb{R}$.*

Now, we can define pullback attractors.

**Definition 2.3** *A family of compact sets $\{\mathscr{A}(t) : t \in \mathbb{R}\}$ is the* pullback attractor for the process *$\{S(t,s) : t \geq s\}$ if*

*i) it is invariant, that is, $S(t,s)\mathscr{A}(s) = \mathscr{A}(t)$ for all $s \leq t$,*

*ii) attracts all bounded subsets of $\mathcal{X}$ in the pullback sense,*

*iii) is minimal in the sense that if there exists a family of closed sets $\{C(t) : t \in \mathbb{R}\}$ such that pullback attracts bounded sets of $\mathcal{X}$, then $\mathscr{A}(t) \subset C(t)$, for all $t \in \mathbb{R}$.*

The above definitions represent one possible way of generalizing the concept of attractor to nonautonomous dynamical systems, see [4, 14].

First, the notion of process is general enough to include smooth nonautonomous dynamical, as well as stochastic processes, e.g. ordinary differential equations with additive noise, see [4, 14].

Also, intuitively, the section (or "slice") $\mathscr{A}(t)$ of a pullback attractor at time $t$ should contain the states seen at time $t$ in an experiment or physical process that had started in the remote past, at $s \to -\infty$. The dependence of the evolution law on time should, in general, make the outcome depend on the "observation time" $t$. Moreover the dissipativity of the system should "collapse" large sets of initial data to a smaller set, contained in $\mathscr{A}(t)$. In the special case of an autonomous system, the process depends only on $t - s$. Then $\mathscr{A}(t)$ is independent of $t$ and coincides with the global attractor of an autonomous system. A related concept of "pushforward", or "future" attractor can be also defined, but seems to be more difficult to handle, e.g. we do not have an analogue of Theorem 2.4 below, see [4, 14] for more information.

In the numerical experiments of Section 4 we will consider integration from a set of initial points $u(s)$ in $X$, starting at a sufficiently negative time $s$, and examining the corresponding trajectories $u(t, s; u(s))$ at $t = 0$. The "asymptotic set" of computed $u(0, s; u(s))$ should approximate a subset of $\mathscr{A}(0)$. In the examples of Section 4, different observation times $t$ seem to give nearby endpoints.

Note that by its definition the pullback attractor can contain nonautonomous analogues of invariant unstable sets and their unstable manifolds. This part of the attractor is examined in more detail in Section 3, but can not be seen directly in simulations. On the other hand, the numerical experiments of Section 4 should be able to detect the parts of the attractor that are locally attracting. We will not formalize here the notion of local attractivity for nonautonomous systems, and we will refer to these sets in Section 4 as "asymptotic states", or "attracting sets".

The following result from [1, 2] gives sufficient conditions for the existence of the pullback attractor.

**Theorem 2.4** *Let $\{S(t, s) : t \geq s\}$ be an evolution process in a metric space $\mathcal{X}$. Then, the following statements are equivalent*

- *$\{S(t, s) : t \geq s\}$ possesses a pullback attractor $\{\mathscr{A}(t) : t \in \mathbb{R}\}$.*
- *There exists a family of compact sets $\{K(t) : t \in \mathbb{R}\}$ that pullback attracts bounded subsets of $\mathcal{X}$ under $\{S(t, s) : t \geq s\}$.*

In the case of system (1) we apply the above framework with $\mathcal{X} = X = \mathbb{C}^N = \mathbb{R}^{2N}$, and $d_{\mathcal{X}}$ the Euclidean norm $\|\cdot\|_X$ in $\mathbb{R}^{2N}$.

We now prove the existence of the pullback attractor for (1). By the theorem above, we need to show the existence of a family of compact absorbing sets in the pullback sense. In this way, we are going to obtain a estimate for the norm of the solution in $X$.

**Proposition 2.5** *System (1) has an absorbing ball $B(0, K_0)$ in $X = \mathbb{C}^N$ that attracts in the pullback sense. Furthermore, system (1) has a pullback attractor $\{\mathscr{A}(t) : t \in \mathbb{R}\} \subset \mathbb{R} \times B(0, K_0)$.*

***Proof:*** Proceeding as in (4) for $u_j = (u(t,s;u(s)))_j$,

$$\begin{aligned}\frac{d}{dt}\sum_{j\in J}|u_j|^2 &= 2\sum_{j\in J}\left(V_j|u_j|^2 - \varepsilon|u_j|^4\right) + 2\sum_{j\in J}\mathrm{Re}\ (\overline{g_j(t)}u_j)\\ &\leq 2\sum_{j\in J}\big((V_j+1)|u_j|^2 - \varepsilon|u_j|^4\big) + 2\sum_{j\in J}|g_j(t)|^2\\ &\leq 2\sum_{j\in J}\big((V_j+1)|u_j|^2 - \varepsilon|u_j|^4\big) + 2\sum_{j\in J}K_j^2,\end{aligned}$$

Defining $\alpha$ as in (4),

$$\frac{d}{dt}\sum_{j\in J}|u_j|^2 \leq -2\alpha\sum_{j\in J}|u_j|^2 + 2\sum_{j\in J}\left((V_j+\alpha+1)|u_j|^2 - \varepsilon|u_j|^4\right) + 2\sum_{j\in J}K_j^2.$$

By $-ax^2+bx \leq \frac{b^2}{4a}$, $\forall x\in\mathbb{R}$,

$$\frac{d}{dt}\sum_{j\in J}|u_j|^2 \leq -2\alpha\sum_{j\in J}|u_j|^2 + \frac{1}{2\varepsilon}\sum_{j\in J}(V_j+\alpha+1)^2 + 2\sum_{j\in J}K_j^2,$$

and by Gronwall's Lemma,

$$\sum_{j\in J}|u_j|^2 \leq e^{-2\alpha(t-s)}\sum_{j\in J}|u_j|^2 + \frac{1}{2\varepsilon}\sum_{j\in J}(V_j+\alpha+1)^2 + 2\sum_{j\in J}K_j^2.$$

Therefore, there exists a ball $B(0,K_0)$ of radius

$$K_0 = \frac{1}{2\varepsilon}\sum_{j\in J}(V_j+\alpha+1)^2 + 2\sum_{j\in J}K_j^2,$$

that attracts in the pullback sense.

The existence of the pullback attractor for (1) follows immediately from Theorem 2.4.

□

## 3 Hyperbolic global solution and its unstable set

In this section we discuss some features of the pullback attractor of (1). We will consider the case where the origin of the autonomous version is hyperbolic.

An example of an autonomous system of this type is given by perturbations of the autonomous uncoupled system

$$\dot{u}_j = V_j u_j + (-\varepsilon + ib)|u_j|^2 u_j, \quad j\in J, \tag{6}$$

i.e. (1) with $\gamma = \delta = 0$.

Assuming $J_+ \cup J_- = J$, (6) has solutions of the form

$$u_j(t) \equiv 0, \quad \text{if} \quad V_j < 0; \quad u_j = A_j e^{-i\omega_j t}, \quad \text{if} \quad V_j > 0, \tag{7}$$

with

$$|A_j|^2 = \frac{V_j}{\varepsilon}, \quad \omega_j = -b\frac{V_j}{\varepsilon}. \tag{8}$$

The above solutions lie on the invariant $m-$torus $\mathbf{T}^m(V)$, with $m = |J_+|$. This torus is a normally hyperbolic local attractor for (6).

System (6) also has an hyperbolic equilibrium in $u \equiv 0$: the spectrum $\sigma(V)$ of $V$ does not intersect the imaginary axis and $\sigma^+ = \{\lambda \in \sigma(V) : \text{Re } \lambda > 0\}$ is compact. The unstable manifold is the finite dimensional polydisc $\Pi_{j=1}^m \mathbb{D}_j^2$, where $\mathbb{D}_j^2 = \{z \in \mathbb{C} : |z|^2 \leq V_j/\varepsilon,\ V_j > 0\}$, and $\partial\Pi_{j=1}^n \mathbb{D}_j^2 = \mathbf{T}^m(V)$. Clearly, $\Pi_{j=1}^n \mathbb{D}_j^2$ is also the global attractor of this uncoupled system. The stable manifold is the set $\{u_j = 0 : j \in \mathbb{Z}, V_j \geq 0\}$.

Furthermore, there exists a projection $Q_0 : X \to X$ defined by

$$Q_0 = Q_0(\sigma^+) = \frac{1}{2\pi i}\int_\theta (\lambda I - V)^{-1} d\lambda, \tag{9}$$

where $\theta$ is a curve in $\rho(V) \cap \{\lambda \in \mathbb{C} : \text{Re } \lambda > 0\}$ ($\rho(V)$ is the resolvent of the operator $V$) oriented counterclockwise and enclosing $\sigma^+$. This projection defines two subspaces $X_0^+ = Q_0 X$ and $X_0^- = (I - Q_0)X$ such that $X = X_0^+ \oplus X_0^-$ and

$$\begin{aligned} \|T_0(t-s)|_{X_0^+}\|_{\mathcal{L}(X_0^+)} &\leq e^{\alpha(t-s)}, \quad t - s \leq 0, \\ \|T_0(t-s)|_{X_0^-}\|_{\mathcal{L}(X_0^-)} &\leq e^{-\alpha(t-s)}, \quad t - s \geq 0, \end{aligned} \tag{10}$$

where $\{T_0(t-s) : t \geq s\}$ is the semigroup associated to the solution of the linear system $\frac{d}{dt}u = Vu$.

In what follows we assume a similar hyperbolicity condition at the origin, that is we assume that there exist a projection $Q : X \to X$, subspaces $Z^+ = QX$, $Z^- = (I - Q)X$, and $\tilde{\alpha} > 0$, such that the semigroup $\{T(t-s) : t \geq s\}$ associated with the solution of $\frac{d}{dt}u = (iC + V)u$ satisfies

$$\begin{aligned} \|T(t-s)|_{Z^+}\|_{\mathcal{L}(Z^+)} &\leq e^{\tilde{\alpha}(t-s)}, \quad t - s \leq 0, \\ \|T(t-s)|_{Z^-}\|_{\mathcal{L}(Z^-)} &\leq e^{-\tilde{\alpha}(t-s)}, \quad t - s \geq 0. \end{aligned} \tag{11}$$

Also, a *global solution* of (1) is a function $\xi : \mathbb{R} \to X$ such that $S(t,s)\xi(s) = \xi(t)$ for all $t \geq s$, $\forall s, t \in \mathbb{R}$. We then have the following.

**Lemma 3.1** *Assume* (11). *Then system* (1) *has a bounded global solution* $u^*(t)$.

Assumption (11) can be easily verified for small coupling. For instance, Gersgorin's Circle Theorem (see e.g. [6]) implies that if $\min\{|V_j - i\delta| : j \in J\} > 2\gamma$, then the number of stable and unstable eigenvalues of the origin is the same as in (6).

In the next section we show examples where by increasing $|\delta|$ ($\gamma = 2\delta$) the number of stable and unstable directions changes. We can still however keep the spectrum sufficiently far from the imaginary axis.

***Proof:*** Let us consider the solution $u(t)$ of (1). By the variation of constants formula and denoting $\mathcal{F}(t,u) = F(u) + G(t)$,

$$u(t) = T(t-s)u(s) + \int_s^t T(t-\theta)\mathcal{F}(\theta, u(\theta))d\theta,$$

where $T(t-s)$ is the semigroup associated to the solution of $\frac{d}{dt}u = (V + iC)u$.

By (11) we have

$$Qu(t) = \int_\infty^t T(t-\theta)Q\mathcal{F}(\theta, u(\theta))d\theta,$$
$$(I-Q)u(t) = \int_{-\infty}^t T(t-\theta)(I-Q)\mathcal{F}(\theta, u(\theta))d\theta.$$

Let us define the functional

$$\mathcal{G}(u)(t) = \int_\infty^t T(t-\theta)Q\mathcal{F}(\theta, u(\theta))d\theta + \int_{-\infty}^t T(t-\theta)(I-Q)\mathcal{F}(\theta, u(\theta))d\theta.$$

A global solution of (1) will exist in small neighborhood of 0 if and only if $\mathcal{G}$ has a unique fixed point in $B(0,\eta) = \{u : \mathbb{R} \to X : \sup\{\|u(t)\|_X : t \in \mathbb{R}\} \leq \eta\}$ for $\eta > 0$ small enough. Let us take $u, v \in B(0,\eta)$. Using the estimate in (3), we have

$$\begin{aligned}\int_\infty^t \|T(t-\theta)Q[\mathcal{F}(\theta,u) - \mathcal{F}(\theta,v)]\|_X d\theta &\leq \int_\infty^t \|T(t-\theta)Q\|_{\mathcal{L}(X)}\|F(u) - F(v)\|_X d\theta \\ &\leq \sqrt{3}(\varepsilon^2 + b^2)\eta\|u-v\|_X \int_\infty^t e^{\tilde{\alpha}(t-\theta)}d\theta \\ &= \frac{\sqrt{3}(\varepsilon^2+b^2)\eta}{\tilde{\alpha}}\|u-v\|_X.\end{aligned}$$

In an analogous way, we also obtain that

$$\int_{-\infty}^t \|T(t-\theta)(I-Q)[\mathcal{F}(\theta,u) - \mathcal{F}(\theta,v)]\|_X d\theta \leq \frac{\sqrt{3}(\varepsilon^2+b^2)\eta}{\tilde{\alpha}}\|u-v\|_X.$$

Therefore, taking $\eta < \frac{\tilde{\alpha}}{2\sqrt{3}(\varepsilon^2+b^2)}$, $\mathcal{G}$ is a contraction map and, by the Banach Fixed Point Theorem, there exists a global bounded solution $u^*(t)$ of system (1) with $\|u^*(t)\|_X \leq \eta$.

□

Changing variables $y(t) = u(t) - u^*(t)$, we can rewrite our original system as

$$\frac{d}{dt}y = \mathcal{B}(t)y + h(t,y), \tag{12}$$

where $DF(\cdot)$ represents the Jacobian matrix of $F$ in $\mathbb{R}^{2N}$, $\mathcal{B}(t) = V + iC + DF(u^*(t))$ and $h(t,y) = F(y + u^*(t)) - DF(u^*(t))y - F(u^*(t))$. The natural generalization of hyperbolicity whithin the

framework of evolution processes can be found in [9]. Denoting by $\{S(t,s) : t \geq s\}$ the evolution process associated to

$$\frac{d}{dt}y = \mathcal{B}(t)y, \tag{13}$$

we say that the linear system (13) has an exponential dichotomy with exponent $\omega > 0$ and bound $M > 0$ at $y \equiv 0$ if there exists a family of projections $\{Q^*(t) : t \in \mathbb{R}\}$ in $X$ such that

i) $S(t,s)Q^*(s) = Q^*(t)S(t,s)$,

ii) the restriction $S(t,s)|_{Q^*(s)X},\ t \geq s$ is an isomorphism of $Q^*(s)X$ onto $Q^*(t)X$,

iii) defining $S(t,s)$ for $t \leq s$ as the inverse of $S(s,t) : Q^*(t)X \to Q^*(s)X$,

$$\begin{aligned} &\|S(t,s)Q^*(s)\|_{\mathcal{L}(X)} \leq Me^{\omega(t-s)}, \quad t-s \leq 0, \\ &\|S(t,s)(I-Q^*(s))\|_{\mathcal{L}(X)} \leq Me^{-\omega(t-s)}, \quad t-s \geq 0. \end{aligned} \tag{14}$$

A global solution $u^*(t)$ of (1) is then a *global hyperbolic solution* if the linearization (13) has an exponential dichotomy.

**Lemma 3.2** *Under the assumptions of Lemma 3.1, there exists a bounded global hyperbolic solution $u^*(t)$ of system (1) with $\omega < \tilde{\alpha}$ and $M > 1$ where $\|u^*(t)\|_X < \eta$, for $\eta > 0$ small enough and for all $t \in \mathbb{R}$.*

The proof of Lemma 3.2 is a direct application of Theorem 7.6.11 in [9].

Whithin the framework of the evolution processes, the unstable and stable manifolds of a solution are defined as families of subsets that depend on time and have the same dynamic properties as in the autonomous case (see [2, 3, 4]).

**Definition 3.3** *The unstable set of an hyperbolic global solution $u^*(t)$ of system (1) is the set*

$$\begin{aligned} W^u(u^*) = \{(s,z) \in \mathbb{R} \times X : &\text{ there exists a global solution } \xi(t) \text{ of } (12) \\ &\text{satisfying } \xi(s) = z \text{ and such that } \lim_{t \to -\infty} \|\xi(t) - u^*(t)\|_X = 0\}. \end{aligned}$$

*The stable set of an hyperbolic global solution $u^*(t)$ of system (1) is the set*

$$\begin{aligned} W^s(u^*) = \{(t_0,z) \in \mathbb{R} \times X : &\text{ there exists a solution } u(t), t \geq t_0, \text{ of } (1) \\ &\text{satisfying } u(t_0) = z \text{ and such that } \lim_{t \to \infty} \|u(t,t_0;z) - u^*(t)\|_X = 0\}. \end{aligned}$$

*We denote by $W^u(u^*)(\tau) = \{z \in X : (\tau,z) \in W^u(u^*)\}$ and $W^s(u^*)(\tau) = \{z \in X : (\tau,z) \in W^s(u^*)\}$ the section of the unstable and stable sets respectively.*

Note that $\sup_{t \in \mathbb{R}} \|u^*(t)\|_X < \infty$ implies $W^u(u^*)(t) \subset \mathscr{A}(t)$.

Also, since $\mathscr{A}(t) \subset B_0(0, K_0)$, $\forall t \in \mathbb{R}$, the pullback attractor is the union of all bounded global solutions (see [4]), that is

$$\mathscr{A}(t) = \{\xi(t) : \xi : \mathbb{R} \to X \text{ is a bounded global solution}\}.$$

We now prove the existence of local stable and unstable sets of $u^*(t)$ as graphs.

Define constants $D, L, \rho > 0$ and $0 < \nu < 1$ such that

$$\begin{aligned} &\frac{\rho M}{\omega} \leq D, && \frac{\rho M}{\omega}(1+L) \leq \nu < 1, \\ &\frac{\rho^2 M(1+L)}{\omega - \rho M(1+M)} \leq L, && \rho M + \frac{\rho^2 M^2 (1+L)(1+M)}{2\omega - \rho M(1+L)} < \omega. \end{aligned} \tag{15}$$

Denote by $\mathcal{LB}^u(D, L)$ the complete space of all bounded and globally Lipschitz continuous functions $\Sigma : \mathbb{R} \times X \to X$ defined as all $(t, y) \mapsto \Sigma(t, Q^*(t)z) \in (I - Q^*(t))X$ satisfying that for all $(t, z, \tilde{z}) \in \mathbb{R} \times X \times X$,

$$\begin{aligned} &\sup\{\|\Sigma(t, Q^*(t)y)\|_X : (y, t) \in X \times \mathbb{R}\} \leq D, \\ &\|\Sigma(t, Q^*(t)z) - \Sigma(t, Q^*(t)\tilde{z})\|_X \leq L\|Q^*(t)(z - \tilde{z})\|_X. \end{aligned}$$

Let $\mathcal{LB}^s(D, L)$ be the complete space of all bounded and globally Lipschitz continuous functions $\Sigma : \mathbb{R} \times X \to X$, defined as all $(t, y) \mapsto \Sigma(t, (I - Q^*(t))z) \in Q^*(t)X$ satisfying that for all $(t, z, \tilde{z}) \in \mathbb{R} \times X \times X$,

$$\begin{aligned} &\sup\{\|\Sigma(t, (I - Q^*(t))y)\|_X : (t, z) \in X \times \mathbb{R}\} \leq D, \\ &\|\Sigma(t, (I - Q^*(t))z) - \Sigma(t, (I - Q^*(t))\tilde{z})\|_X \leq L\|(I - Q^*(t))(z - \tilde{z})\|_X. \end{aligned}$$

**Proposition 3.4** *Under the assumptions of Lemma 3.2, the local unstable set $W^u_{loc}(u^*)(t)$ and the local stable set $W^s_{loc}(u^*)(t)$ of (1) are given by a graph, that is there exist $\Sigma^{u,*}(t, \cdot) \in \mathcal{LB}^u(D, L)$ and $\Sigma^{s,*}(t, \cdot) \in \mathcal{LB}^s(D, L)$ a such that*

$$W^u_{loc}(u^*)(t) = W^u(u^*)(t) \cap \mathcal{V}(t) = \{u^*(t) + z + \Sigma^{u,*}(t, z)), z \in Q^*(t)X\} \cap \mathcal{V}(t),$$

*and*

$$W^s_{loc}(u^*)(t) = W^s(u^*)(t) \cap \mathcal{V}(t)\{z + (\Sigma^{s,*}(t, z), z \in (I - Q^*(t))X\} \cap \mathcal{V}(t),$$

*where $\mathcal{V}(t)$ is a neighborhood of $u^*(t)$.*

***Proof:*** In order to prove the existence of the stable and unstable sets of $u^*(t)$ we use the results in [3] (see also [4]). We define $y^+ = Q^*(t)y$ and $y^- = (I - Q^*(t))y$, where $y(t)$ is the solution of (13). These functions $y^+$ and $y^-$ verify for the following systems,

$$\begin{aligned} \dot{y}^+ &= \mathcal{V}^+(t)y^+ + H(t, y^+, y^-), \\ \dot{y}^- &= \mathcal{V}^-(t)y^- + G(t, y^-, y^-), \end{aligned} \tag{16}$$

where

$$\begin{aligned} &\mathcal{V}^+(t) = (V + iC + DF(u^*(t)))Q^*(t), \qquad \mathcal{V}^-(t) = (V + iC + DF(u^*(t)))(I - Q^*(t)), \\ &H(t, y^+, y^-) = Q^*(t)[F(y^+ + y^-) - DF(u^*(t))(y^+ + y^-) - F(u^*(t))], \\ &G(t, y^+, y^-) = (I - Q^*(t))[F(y^+ + y^-) - DF(u^*(t))(y^+ + y^-) - F(u^*(t))]. \end{aligned}$$

For a given $\rho > 0$, there exists a $r > 0$ such that if $\|y\|_{l^2} = \|y^+ + y^-\|_{l^2} < r$,

$$\begin{aligned} &\|H(t, y^+, y^-)\|_{l^2} < \rho, \quad \|G(t, y^+, y^-)\|_{l^2} < \rho \\ &\|H(t, y_1^+, y_1^-) - H(t, y_2^+, y_2^-)\|_{l^2} \leq \rho(\|y_1^+ - y_2^+\|_{l^2} + \|y_1^- - y_2^-\|_{l^2}) \\ &\|G(t, y_1^+, y_1^-) - G(t, y_2^+, y_2^-)\|_{l^2} \leq \rho(\|y_1^+ - y_2^+\|_{l^2} + \|y_1^- - y_2^-\|_{l^2}). \end{aligned} \tag{17}$$

Then, by Theorem 8.4 and 8.5 in [4] we can write the local stable and unstable set of the trivial solution $y \equiv 0$ of system (12) as a graph.

□

# 4 Numerical examples of attracting sets

We consider numerical solutions of system (1) in the autonomous and nonautonomous cases. We will show evidence for the existence of multiple localized asymptotic states for the autonomous system, and their persistence under nonautonomous perturbations.

We set $\delta = 2\gamma$, so that the operator $C$ is the second order finite difference discrete (Dirichlet) Laplacian. $\delta$ is then the intersite coupling constant. We also fix $b = 2$, $\varepsilon = 0.01$, and consider a lattice with $N = 19$ sites.

We will generally force a few sites at the center of the lattice, and damp all other sites.

The linear stability of the origin is determined by the spectrum of $V + iC$, and some examples are shown in Figures 1, 2.

The spectra of Figure 1 correspond to a realatively weakly damping (see caption). The damping can be stronger or comparable to the coupling constant $|\delta|$. Increasing $|\delta|$ increases the imaginary part of the eigenvalues, moreover as $|\delta|$ becomes comparable to the damping, the hyperbolicity condition becomes harder to satisfy, as many eigenvalues pass to the right of the imaginary axis, i.e. compare Figures 1 (a), (b).

In Figure 1 (a) the coupling is weaker than the damping. The forcing is such that frequencies of the uncoupled nonlinear oscillators of the forced sites, see (8), are large compared to the coupling. The forced sites then have approximate periodic motions, and seem to evolve independently from each other. This seems to be a more tractable regime analytically and will be studied elsewhere.

In Figure 2 we use stronger damping, so that we can also use a stronger coupling and still keep the condition of hyperbolicity at the origin. In Figures 2 (a), (b) we see that we can increase the coupling parameter and keep the eigenvalues away from the imaginary axis. The number of unstable eigenvalues in Figures 2 (a), (b) is 6. In Figure 2 (c) we have larger coupling, $\delta = -1.0$, and the number unstable eigenvalues is 4. The eigenvalues are still relatively far from the imaginary axis, i.e. compare to Figure 1 (b).

In the autonomous case, the dynamics corresponding to the parameters of Figures 2 (b), (c), i.e. weaker and stronger coupling respectively, are different.

In Figure 3 we show the asymptotic profile of the mode amplitudes for the weaker coupling $\delta = -0.4$ of Figure 2 (b). The asymptotic profile shown in Figure 3 is typical: we used 100

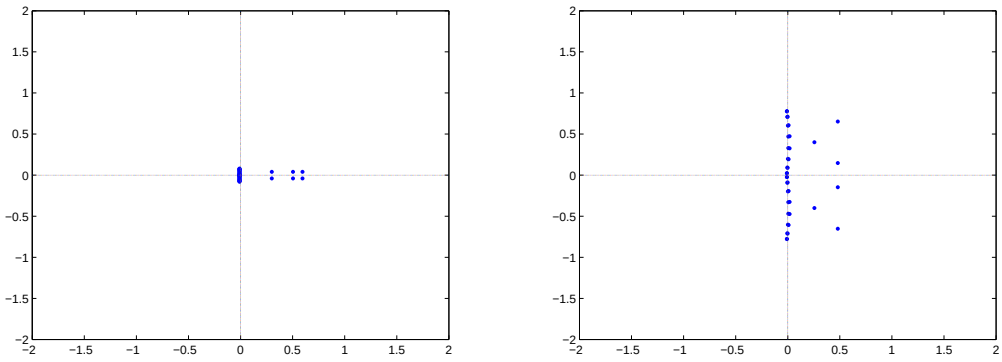

(a) (b)

Figure 1: (color online) Spectrum of $V + iC$ for different values $\delta$, for $N = 19$ sites, and $\delta = 2\gamma$, $V_9 = 0.5$, $V_{10} = 0.6$, $V_{11} = 0.3$, $V_j = -0.01$, $j \notin I = \{9, 10, 11\}$. (a) $\delta = -0.02$. Eigenvalues are near the values of the $V_j$: 6 eigenvalues with positive real part, all other eigenvalues have real part below $-0.005$ (b) $\delta = -0.2$. 22 unstable eigenvalues, 6 with real part above 0.25 (real parts are close to $V_j$, $j \in I$, to whithin 20%), other unstable eigenvalues have real part below 0.181.

pseudorandom initial conditions with power $P = 160$ (generated as described in [12]) and saw in all cases convergence to the amplitude profile shown in Figure 3. In all examples the power approached an approximate value $140.0 \pm 0.1$, while the amplitudes of the forced modes apporached an almost constant value, with a small time variation of at most 5% of what we see in the figure.

In Figure 4 we see results from a similar experiment, using instead the stronger coupling $\delta = -1.0$, as in Figure 2 (c). All initial conditions lead to asymptotic states of slowly varying total power and mode amplitudes, as in Figure 3. Here however we see several different asymptotic amplitude profiles. There is thus evidence of several attracting sets and multistability.

We have so far detected at least 5 different possible attractors. Most initial conditions (about 90%) asymptote to an attractor localized in the three forced modes $n = 9$, 10, 11, as seen in Figure 4 (a). Figures 4 (b), (c), (d) show three less common asymptotic profiles. In Figure 4 (b) we see that the site $n = 8$ is also excited. Figures 4 (c), (d) show localization at two sites. In Figure 4 (d) the amplitudes at $n = 9$, and 10 approach a constant common value.

The asymptotic amplitude profiles shown above have been observed with different integrators and time steps. In Figure 4 (d) we see some evidence for phase locking between $u_9(t)$ and $u_{10}(t)$. This fact is however only observed using a higher order integrator such as a sixth-seventh order variable step Runge-Kutta. A fourth order Runge-Kutta with timestep $10^{-4}$ shows the same asymptotically constant amplitudes at $n = 9$, 10, but no phase locking.

Note that (1) can in principle have solutions of the "breather" form $u_n = e^{i\omega t} A_n$, with $\omega$ real, and $A_n$ independent of time. These can be obtained by first finding breather solutions of the Hamiltonian system (1) with $V = 0$, $\epsilon = 0$, and choosing appropriate $V$, see e.g. [10]. Their existence for generic $V$ does not seem obvious.

The above attractors do not seem to be periodic. Evidence for this comes from projections of

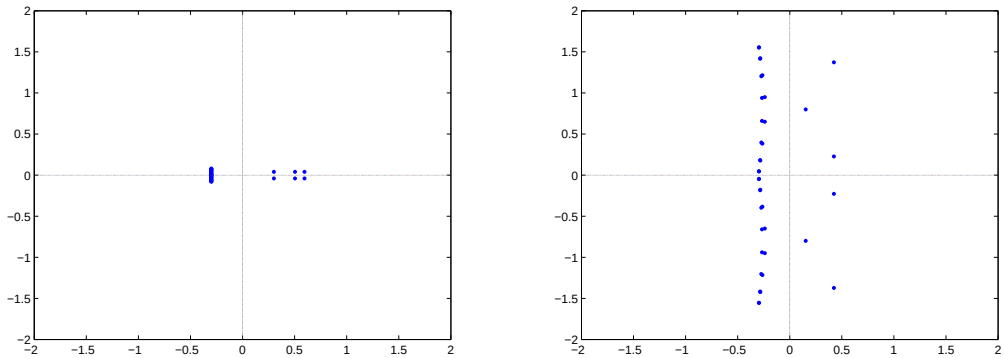

(a) (b)

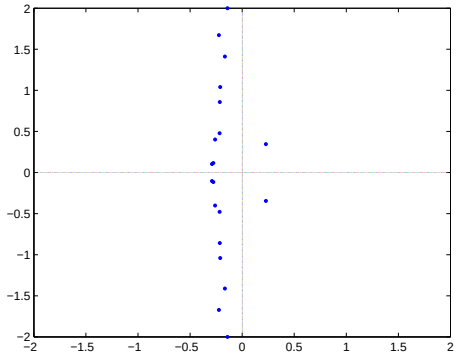

(c)

Figure 2: (color online) Spectrum of $V + iC$ for different values $\delta$, for $N = 19$ sites, and $\delta = 2\gamma$, $V_9 = 0.5$, $V_{10} = 0.6$, $V_{11} = 0.3$, $V_j = -0.3$, $j \notin I = \{9, 10, 11\}$. (a) $\delta = -0.02$. Eigenvalues are near the values of the $V_j$: we have 6 eigenvalues with positive real part, all other eigenvalues have real part below $-0.26$. (b) $\delta = -0.4$ Real parts of eigenvalues realatively near the values of the $V_j$, larger imaginary parts. Number of stable and unstable directions as in (a). (c) $\delta = -1.0$, 4 unstable eigenvalues (two conjugate pairs that are very close), all other eigenvalues have real part below $-0.4$.

the points on the attractor to planes, checking for recurrences, and from Fourier spectra.

In the examples shown in Figure 4, the Fourier transform of the $u_j(t)$, at the sites $j$ of largest amplitude, is strongly peaked. For instance the Fourier transforms of (real and imaginary parts of) $u_9(t)$, $u_{10}(t)$, and $u_{11}(t)$ from Figure 4 (a), are strongly peaked at $\omega_9 = 106.8993$, $\omega_{10} = 106.8993$, and $\omega_{11} = 58.3392$ respectively. We thus see both resonance, and possibly incommensurate frequencies. For instance, we have $|k_1\omega_{10} + k_2\omega_{11}| > 10^{-6}$, for all integers $|k_1|$, $|k_2| \leq 1000$; this implies a lower bound on a possible period $T > 1000(2\pi/\omega_{10}) \sim 58.7$ (for motion on a torus with these frequencies).

In the attractor of Figure 5 (b), $u_8(t)$, $u_9(t)$, $u_{10}(t)$ and $u_{11}(t)$ have spectra peaked at $\omega_8 = 17.0655$, $\omega_9 = 17.0655$, $\omega_{10} = 117.9727$, and $\omega_{11} = 58.0036$ respectively. and we have 2 possibly

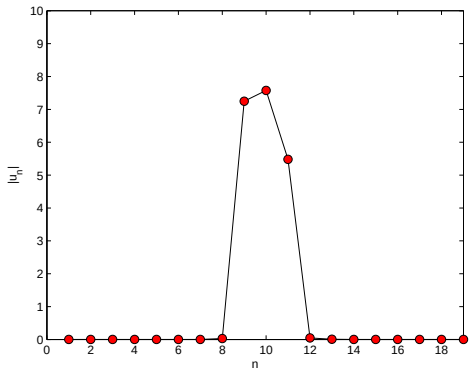


(a)

Figure 3: (color online) Amplitude $|u_n|$ v.s. $n$ at time $t = 0$, integration interval $[-400, 0]$ for autonomous system with parameters of Figure 2 (b), i.e. coupling $\delta = -0.4$. The amplitude shown is typical for 100 initial conditions considered. The modes $u_9$, $u_{10}$, $u_{11}$ oscillate with approximately constant amplitudes near those shown in the figure: $|u_9| = 7.1 \pm 0.3$, $|u_{10}| = 7.6 \pm 0.3$, $|u_{11}| = 5.6 \pm 0.2$, for all initial conditions.

incommensurate frequencies. For instance, we have either $|k_1\omega_9 + k_2\omega_{10}| > 10^{-6}$, for all integers $|k_1|, |k_2| \leq 1000$, or $|m_1\omega_{10} + m_2\omega_{11}| > 10^{-6}$, for all integers $|m_1|, |m_2| \leq 1000$; this implies a lower bound on a possible period $T > 1000(2\pi/\omega_{10}) \sim 53.2$ (for motion on a torus with these frequencies). Also, these frequencies are far from the ones predicted for the uncoupled system, see (8).

Small nonautonomous perturbations of additive type of the system of Figures 3, 4 do not seem to affect the presence of multiple, well localized asymptotic states, although they can alter the basins of attraction, and make some asymptotic states unobservable.

Figures 5 (a), (b) shows asymptotic amplitude profiles at $t = 0$ for the system of Figure 4 with a nonautonomous perturbation, see caption of Figure 5. The initial time was $s = -400$. The justification for considering $s = -400$ sufficiently negative is the observed convergence of the power $P$ and the amplitudes $|u_j|$ to approximately constant values at about $t = -200$. In Figure 5 (a) we see an amplitude profile that is close to that of Figure 4 (a), it is obtained however from the initial condition of Figure 4 (c). In Figure 5 (b) we start with the initial condition of Figure 4 (b), and obtain a similar localized profile.

Figure 6 compares the Fourier spectra of the higher amplitude modes in the autonomous and nonautonmous cases, seen in Figures 4 (b), and 5 (b) respectively. They are in both cases strongly peaked, with some slight differences in the peak frequencies seen at some sites.

The simulations of Figure 5 used periodic, and "chaotic" additive perturbations, with $g_j$ nonzero only at the endpoints $j = 1, 19$ of the lattice. We typically have $\sup_t |g_j(t)| \leq 2$, $j = 1, 19$. This forcing is not small but is not transmitted efficiently to the forced sites at the center of the lattice. Note that the "chaotic" perturbation, e.g. the function $f$ in the caption of Figure 5, is a component of a numerical trajectory of the Hamiltonian discrete NLS equation discussed in [13]. We used parameter values for which the numerical trajectories exhibit fast "equipartition of

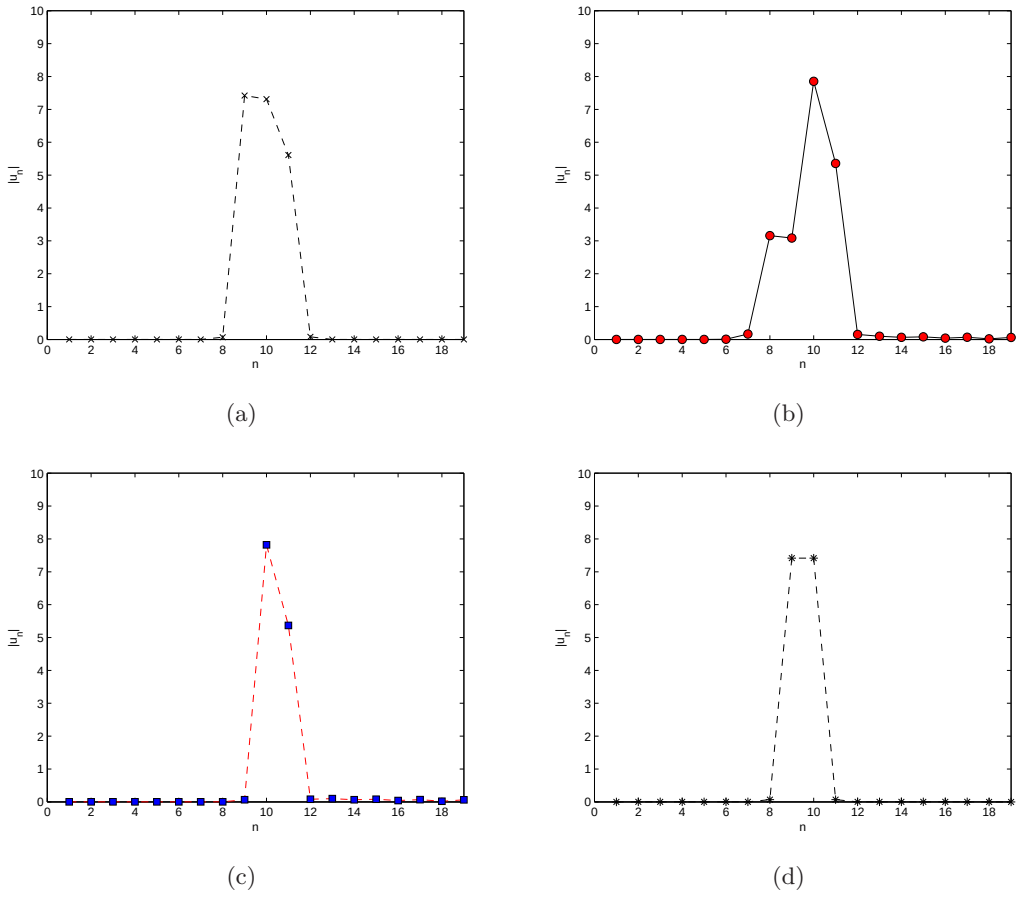


Figure 4: (color online) Figures 4 (a), (b), (c), (d) show amplitudes $|u_n|$ v.s. $n$ at time $t = 0$ obtained from three different initial conditions for autonomous system with the parameters of Figure 2 (c), i.e. coupling $\delta = -1.0$. The integration interval was $[-400, 0]$. For large times the mode amplitude oscillate slightly around the values shown in the figure. (a) Asymptotic state localized in three sites. (b) Asymptotic state localized in four sites. (c) Asymptotic state localized in two sites. (d) Asymptotic state localized at sites $n = 10$, 11, mode amplitudes at these sites approach equal, constant values.

power", as well as significant loss of accuracy for longer time scales, of the order 100. This possible chaoticity of the underlying system (combined with the likely lack of accuracy over the time scale used in the simulations here) is considered an advandage for our purposes.

In the experiments reported here it is generally seen that the computed subsets of the sections $\mathscr{A}(t)$ of the pullback attractor at different final times $t$ are not significantly different. This is likely related to the oscillatory nature of the forcing we have used. The observations then give possibe examples where the sections $\mathscr{A}(t)$ of the pullback attractor have the same topology, $\forall t \in \mathbb{R}$.

We have also seen possible examples where the sections $\mathscr{A}(t)$ of the pullback attractor of the nonautonomously perturbed system have the structure of the attractor of the autonomous system; this seems to be the case for small nonautonomous perturbations of the system of Figure 3. The

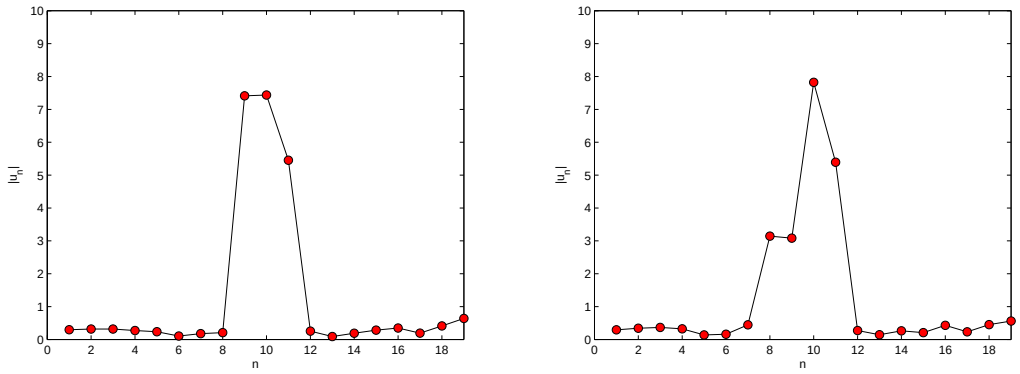


(a) (b)

Figure 5: (color online) Figures 5 (a), (b) show amplitudes $|u_n|$ v.s. $n$ at time $t = 0$ obtained from two different initial conditions for nonautonomous system with the parameters of Figure 2 (c), i.e. coupling $\delta = -1.0$ with added forcing $g_1(t) = \sin t$, $g_{19}(t) = \cos(2.5t) + f(t)$, where $f(t)$ is a "chaotic signal" satisfying $|f(t)| \leq 1$, $\forall t$, and $g_j \equiv 0$, otherwise. The integration interval was $[-400, 0]$. The mode amplitude oscillate slightly around the values shown in the figure, for both (a), (b).

perturbations of the autonomous system of Figure 4 shown in Figure 5 may give an example where the $\mathscr{A}(t)$, assumed to have the same topology for all $t$, are different from the attractor of the autonomous system, for instance in the experiments of Figure 5 we do not see the asymptotic state of Figure 4 (d).

## 5 Discussion

We have studied some basic properties of attractors in a spatially forced and damped discrete NLS model. We have seen that the system can have multiple nontrivial attractors that persist under nonautonomous perturbations of additive type.

The proposed model has a limit, namely the uncoupled case $\delta = \gamma = 0$, where the asymptotic dynamics takes place on normally hyperbolic tori. Our study motivates more detailed studies of these invariant tori and their internal dynamics, in both the autonomous and nonautonomous cases. For larger intersite coupling we see evidence of qualitative changes in the asymptotic dynamics that should be examined in more detail, in both the autonomous and nonautonomous cases.

Also of interest is a study of more general nonautonomous perturbations, such as small perturbations of the system parameters, as well as cases where the hyperbolicity at the origin does not hold for all times.

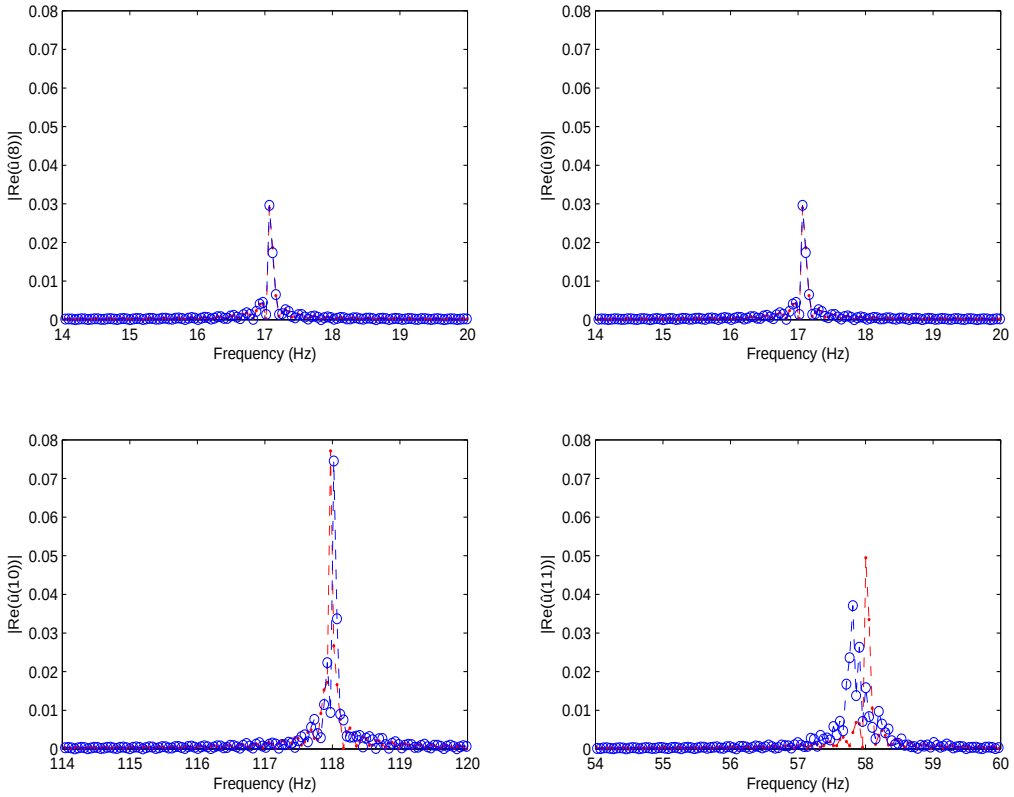


Figure 6: (color online) Superposed Fourier (power) spectra of $\mathrm{Re}(u_n(t))$ v.s. $\omega$ (frequency) from autonomous, and nonautonomous trajectories, at sites $n = 8$ (a), 9 (b), 10 (c), 11 (d). Circles show data corresponding to Figure 4(b) (autonomous), dots show data corresponding to Figure 5(b) (nonautonomous). In all cases we Fourier transform $\mathrm{Re}(u_n(t))$, $t \in [-100, 0]$; integration starts at $t_0 = -400$. Power spectra look identical at $n = 8$, 9, small changes in peak frequencies at $n = 10$, and especially at $n = 11$.


### Acknowledgments

We thank A. Aceves for helpful discussions. P. Panayotaros acknowledges partial support from Conacyt 177246, and FENOMEC. F. Rivero acknowledges partial support from MEC grant MTM 2011-22411.


## References


[1] T. Caraballo, A.N. Carvalho, J.A. Langa, F. Rivero, Existence of pullback attractors for pullback asymptoticaly compact processes, Nonlinear Anal. 72, 1967-1976 (2010)

[2] T.Caraballo, A.N. Carvalho, J.A. Langa, F. Rivero, A gradient-like nonautonomous evolution process, Int. J. of Bifurcation and Chaos 20, 9, 2751-2760 (2010)

[3] A.N. Carvalho, J.A. Langa, Non-autonomous perturbation of autonomous semilinear differential equations: Continuity of local stable and stable manifolds, J. Diff. Equations 233, 622-653 (2007)

[4] A.N. Carvalho, J.A. Langa, J.C. Robinson, *Attractors for infinite-dimensional non-autonomous dynamical systems*, Springer, New York (2013)

[5] D. N. Christodoulides, R. I. Joseph, Discrete self-focusing in nonlinear arrays of coupled waveguides, Opt. Lett. 18, 794 (1988)

[6] S.Gersgorin, Über die Abgrenzung der Eigenwerte einer Matrix, Izv. Akad. Nauk. USSR Otd. Fiz.-Mat. Nauk7 74-754 (1931)

[7] J.K. Hale, *Asymptotic Behavior of Dissipative Systems*, A.M.S., Providence (1989)

[8] P. Hartman, *Ordinary Differential Equations*, SIAM (2002)

[9] D. Henry, *Geometry Theory of Semilinear Parabolic Equations*, Springer, New York (1981)

[10] Y.V. Kartashov, V.V. Konotop, V.A. Visloukh, Two-dimensional dissipative solitons supported by localized gain, Opt. Lett. 36, 82 (2011)

[11] C.K. Lam, B.A. Malomed, K.W. Chow, P.K.A. Wai, Spatial solitons supported by localized gain in nonlinear optical waveguides, Eur. Phys. J. Special Topics 173, 233-243 (2009)

[12] P. Panayotaros, A. Aceves, Stabilization of coherent breathers in perturbed Hamiltonian coupled oscillators, Phys. Lett. A 375, 45, 3964-3972 (2011)

[13] P. Panayotaros, Continuation of normal modes in finite NLS lattices, Phys. Lett. A 374, 38, 3912-3919 (2010)

[14] M. Rasmussen, *Attractivity and bifurcation for nonautonomous dynamical systems*, Lect. Notes Math. 1907, Springer, New York (2007)

[15] M.O. Williams, C.W. McGrath, J.N. Kutz, Light-bullet routing and control with planar waveguide arrays, Opt. Express 18, 11671 (2010)

[16] D.V. Zezyulin, V.V. Konotop, Nonlinear modes in finite-dimensional PT-symmetric systems, Phys. Rev. Lett 108, 213906 (2012)